energies

MDPI

Article

Experimental Investigation of Displacer Seal Geometry Effects in Stirling Cycle Machines

Jan Sauer and Hans-Detlev Kühl *

TU Dortmund University, Lehrstuhl für Thermodynamik (BCI), Emil-Figge-Straße 70, 44227 Dortmund, Germany; jan.sauer@tu-dortmund.de

* Correspondence: hans-detlev.kuehl@tu-dortmund.de; Tel.: +49-231-755-2674

Received: 22 August 2019; Accepted: 30 October 2019; Published: 5 November 2019

Abstract: This contribution deals with an experimental investigation of the optimization potential of Stirling engines and similar regenerative machines by an enhanced design of the cylinder liner and the seal. The latter is mounted at the bottom end of the gap surrounding pistons and displacers that separate cylinder volumes at different temperature levels. The thermal loss associated with this gap may amount to more than 10% of the heat input into these machines. Mostly, its design is reduced to an estimation of the optimum width by analytical models, which usually do not account for further relevant optimization parameters, such as a step in the cylinder wall. However, a recently developed, enhanced analytical model predicts that this loss may be significantly reduced by such a step. In this work, this design was realized and investigated experimentally according to this prediction by modification of the cylinder liner and the seal of an extensively tested laboratory-scale machine. The results confirm that such a design actually reduces the thermal loss substantially, presumably by reducing the cyclic mass flows through the open end of the gap. Additionally, it even improves the net power output due to a reduced volumetric displacement by the piston or displacer, resulting in smaller flow losses and thermal regenerator losses, whereas the pressure amplitude remains virtually unchanged, contrary to initial expectations. This has led to the remarkable conclusion that the design of most Stirling engines is possibly suboptimal in this respect and may be improved a posteriori by a minor modification; i.e., a reduction of the effective displacer seal diameter.

Keywords: Stirling engine; experimental results; appendix gap loss

1. Introduction

The so-called regenerative gas cycles constitute a promising class of thermodynamic cycles capable of performing energy conversion in heat engines or heat pumps at high efficiency, since the underlying ideal cycles are theoretically reversible. In particular, the most well-known representative, the Stirling cycle, has gained increasing interest in the field of decentralized cogeneration, solar power, or refrigeration applications, and consequently, much development work has been done in recent years [1–10]. Similar regenerative cycles, such as the Vuilleumier cycle, are of interest for domestic heat pump applications [11–14]. However, the actual machine performance is substantially degraded by various loss mechanisms, which highly depend on the details of the machine design. The so-called appendix gap loss, a severely design-dependent and significant thermal loss that may easily amount to more than 10% of the heat input to Stirling engines or Vuilleumier heat pumps, is associated with the annular gap surrounding pistons and displacers. Usually, it is either evaluated using separate analytical models for the two major underlying mechanisms, the so-called shuttle-loss [15,16] and the so-called enthalpy loss [17,18], or by numerical simulation [19–24]. Particularly in the case of free piston machines featuring close tolerance seals rather than sliding seals, leakage losses need to be considered additionally [25]. However, this case is excluded within the scope of this contribution. According to

recent investigations based on an enhanced analytical model [26,27], the appendix gap loss may be substantially reduced if the design optimization is not confined to the gap width h only, but is further extended to additional parameters, such as the conicity of the cylinder wall or the diameter of the seal and the cylinder liner, which may possibly deviate from the internal cylinder wall diameter in the gap above. In detail, the latter option implies a step in the cylinder wall and different gap widths in the range of the seal and above. Such a gap design is actually found in the well-documented and extensively tested GPU-3 Stirling engine [28,29], indicating the optimization potential of this design parameter. However, no information about the derivation of the actual appendix gap geometry in the GPU-3 Stirling engine is available. Further experimental studies on such a s step in the cylinder wall or a conicity are not known.

For experimental studies particularly on the effect of a step in the cylinder wall, an existing laboratory-scale machine capable of realizing four different regenerative cycles or operating modes, respectively [30,31], appeared to be very well suited because of this additional degree of freedom primarily affecting the relative amplitude and phase angle of the cycle pressure and because of its exchangeable hot cylinder liner facilitating the realization of such a step. Furthermore, this machine was recently equipped with high-speed thermocouple probes to measure the unsteady gas temperature profiles in the gap and thus verify the aforementioned analytical model experimentally [32]. So, the effect of such a design modification on the engine performance and the gas temperature profiles could be directly studied using this machine.

In the subsequent chapters, the modification of this machine based on the predictions of the analytical model is introduced. Furthermore, the results of stationary heat balance measurements will be presented and contrasted to the old design to demonstrate the positive effect of this design option, which exceeds a pure reduction of the heat loss in the appendix gap. Additionally, the underlying mechanisms, which inter alia affect the loss by pressure drop in the machine and have not been inspected so far, will be analyzed and discussed based on supplementary information such as experimental gas temperature and pressure data.

2. The Appendix Gap Loss and Its Minimization

In general, regenerative gas cycles are characterized by a periodic displacement of the working fluid—typically a gas—between different temperature levels, whereby regenerators act as thermal energy storage, giving this group of cycles its name. Regardless of whether this displacement is performed by a double-acting displacer or a single-acting piston, a thermal insulation is required between different temperature levels, e.g., by a hollow, thin-walled dome mounted on top of the piston separating a hot cylinder volume from the "warm" crank case (reserving the attribute "cold" for a third, typically near-ambient temperature level). For reasons of conciseness, the following considerations are only presented for the case of a displacer separating two cylinder volumes, but they may be applied to pistons as well. The aforementioned thin-walled domes are separated from the cylinder wall by an inevitably emerging gap. Typically, the seal is located at a moderate temperature level to protect it from too-high or too-low temperatures. Thus, the gap is open toward the hot temperature level in the case of heat engines, or toward the cold temperature level in the case of refrigerators. Counteracting the thermal losses in the gap, the bottom section of the gap (at the seal) additionally acts as a heat sink in the case of a heat engine, thus reducing the net heat flow to the adjacent volume. However, this heat pump effect is of course only possible at internal cost; i.e., a reduction of available work.

In detail, the enthalpy loss is caused by cyclic density fluctuations in the gap, generating an oscillating mass flow at the open end. In a simplified view for the exemplary case of a heat engine, hot gas flowing into the gap from the cylinder volume is cooled to some extent, leaving the gap at a lower temperature. This results in a net enthalpy flow, which is linearly dependent on the gap width h. In contrast, the shuttle loss is caused by a cyclic relative displacement between the axial temperature profiles in the cylinder and the displacer wall. This results in a cyclic radial heat exchange between the walls, which is essentially limited by the gas in the gap acting as an insulating layer due

to its finite thermal conductivity. Thus, the shuttle loss features a reciprocal dependency on the gap width. This loss may also be regarded as a net enthalpy flow in the axial direction provided by the solid matter of the moving displacer wall. Obviously, these losses feature opposite dependencies on the gap width, and thus, an optimum gap width yielding the lowest sum of losses must be found. This, however, requires an accurate modeling of the loss mechanisms. Mostly, the losses are estimated based on simplified analytical models; i.e., the models by Rios [15] and Chang, et al. [16] for the shuttle loss and the models by Berchowitz [17] and Magee and Doering [18] for the enthalpy loss. Thermal conduction in the walls is then simply superimposed to the analytical results, neglecting mutual interactions between the losses and the wall temperatures. However, an extensive review [33] has revealed that some of the assumptions in the common models are questionable and thus gave rise to the development of the aforementioned analytical model [26] and the subsequent optimization of the gap and seal geometry by Pfeiffer and Kühl [27]. For the exemplary case of the GPU-3 Stirling engine, they predict that an optimization of the conicity and the seal diameter, in combination with the gap width, may yield a further reduction of the appendix gap loss by 15% compared to an optimization of the gap width only, without a step or a conicity in the cylinder wall. Finally, they suggest maximizing the step in the cylinder wall, corresponding to a seal that is fixed to the cylinder and runs on the displacer surface.

3. Seal Design Modification in the Convertible Laboratory-Scale Machine

The aforementioned laboratory-scale machine may be operated in four different modes, realizing two variants of a γ-Stirling cycle, a thermally driven Vuilleumier heat pump cycle, and a so-called hybrid cycle featuring both a net power output and a heat pump effect. It was developed to demonstrate that such a system may be designed for a satisfactory performance in any of those modes and may therefore be profitably used as a domestic tri-generation system, which can be toggled in a demand-dependent way [30,31]. The design of the laboratory-scale machine depicted in Figure 1 was derived from an original, application-oriented design [34] by a similarity-based scaling procedure, thus reducing operating and manufacturing costs in the project [35,36].

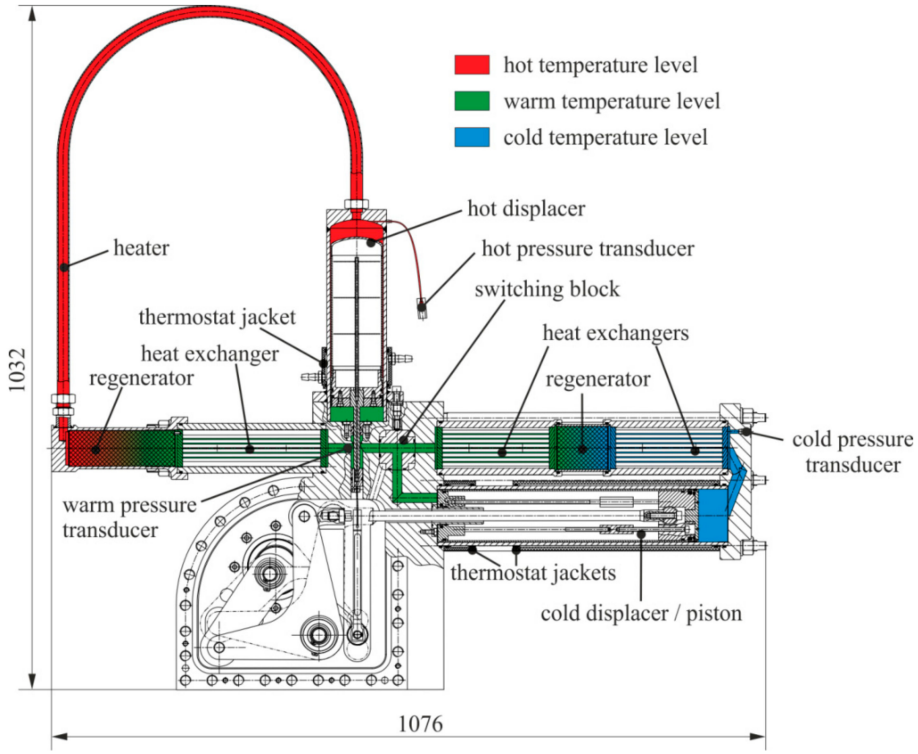

Figure 1. Cross-section of the laboratory-scale machine without fine-wire thermocouple probes.

So, this merely experimental machine is apparently impractical, featuring, e.g., a single heater tube only, which is heated electrically for reasons of simplicity and better balancing. Due to the scaling procedure, it also features extended surfaces and an oversized crank mechanism compared to its low power density, and therefore any heat flows and net power data collected during an extensive test program had to be corrected for size-dependent losses [13]. Furthermore, the width of the appendix gap, which was determined based on the analytical models by Rios [15] and Berchowitz [17], amounts to 1.4 mm in the case of the hot displacer because of the scaling. Due to this large width, it was possible to equip the gap section with fine-wire thermocouple probes for high-speed gas temperature measurements within a subsequent project [32]. These probes are radially adjustable over the entire gap width by a micrometer head. However, no measurements close to the displacer wall are possible due to the risk of destroying the probes. The gas temperatures are measured by a fine-wire thermocouple mounted on top of two supporting wires, made of the same alloy as the corresponding wire of the fine-wire thermocouple. Furthermore, the machine was equipped with a series of wall thermocouples along the hot cylinder wall, as well as a third pressure transducer attached to the hot cylinder volume, thus ensuring a precise evaluation of the indicated work. Detailed information concerning the new instrumentation is provided in [32]. To ensure similarity with respect to thermal conduction and appendix gap losses, thermostat jackets are attached to the hot and cold displacers. Toggling between the operating modes is realized by a switching block, which disconnects different volumes at the cold displacer/piston. In Vuilleumier mode, all cylinder volumes are connected to the internal cycle and the machine acts as a thermally driven heat pump at the three temperature levels indicated by different colors in Figure 1. In Stirling mode, the volume on the "left" side of the cold displacer is disconnected and ventilated to the crank case instead. Additionally, the cold regenerator is thermally bypassed by adapting the cold temperature level T_c to the warm temperature level T_w. The remaining operating modes have not been used for the investigations reported here and are therefore not explained in detail.

Figure 2 shows a cross-sectional view of the hot cylinder system, including positions of the thermocouple probes. Based on the analytical results by Pfeiffer and Kühl [27], the seal design of the hot displacer was modified by a reduced diameter of the cylinder liner for this study. The resulting step in the cylinder wall above the seal is also illustrated in Figure 2, along with the initial design, which is indicated by dashed double dotted lines. These will be addressed as the "new" and the "old" seal design in the following: The size of this step is quantified by the gap width ratio

$$r_h = \frac{h_0}{h}\,, \tag{1}$$

where h_0 designates the gap width at the seal. It is generally dependent on the specific machine design and the operating conditions. However, since no closed form equations for the optimum gap width ratio are available yet, it has to be determined by numerical minimization of the calculated appendix gap loss given by the analytical model by Pfeiffer and Kühl [27]. For reasons of clarity, the corresponding extensive equations will not be reproduced in this contribution. The optimum gap width ratio for the experimental machine is predicted as $r_h = 0.1$ in Stirling mode and $r_h = 0.2$ in Vuilleumier mode, respectively. Thus, for constructive reasons, the new gap width at the seal was chosen as the minimum feasible gap width $h_0 = 0.3$ mm, which results in a gap width ratio $r_h = 0.21$. For this value, the analytical model predicts a reduction of the appendix gap loss by 297 W and 223 W in Stirling mode and Vuilleumier mode, respectively.

The nominal operating conditions of the laboratory-scale machine, as well as the major geometric dimensions concerning the hot displacer and the appendix gap section are summarized in Table 1. Evidently, the seal diameter is reduced from 80 mm to 77.8 mm in the new design, thus decreasing the volumetric displacement correspondingly.

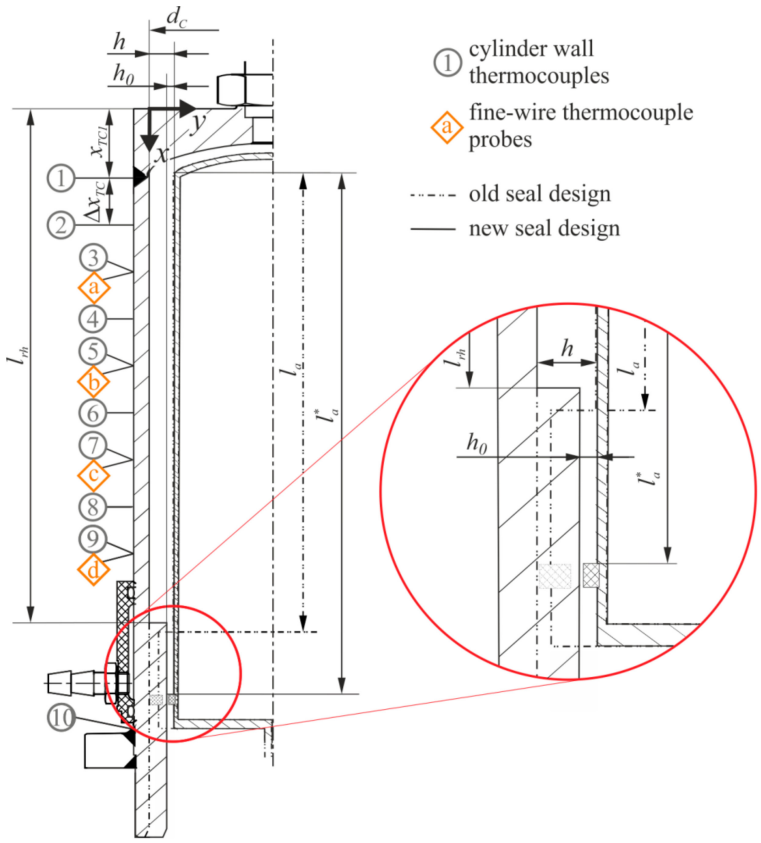

Figure 2. Axial positions of fine-wire and wall thermocouples and illustration of old seal design (dashed double dotted lines) and new seal design.

Table 1. Nominal operating conditions and geometric dimensions of the laboratory-scale machine[1].

Parameter	Value	Parameter	Value
Heater temperature T_h	500 °C	Displacer stroke amplitude	21.75 mm
Intermediate temperature T_w	30 °C	Old appendix gap length l_a	201 mm
Cold temperature T_c (Vuilleumier mode)	10 °C	New appendix gap length $l_a{}^*$	227 mm
Working fluid	Helium	Appendix gap width h	1.4 mm
Rotational speed n	383 min^{-1}	Bottom gap width h_0	0.3 mm
Mean pressure $\overline{p}$	38.3 bar	Axial position of step l_{rh}	240 mm
Cylinder internal bore	80 mm	Axial position of thermocouple 1 x_{TC1}	30 mm
Cylinder wall thickness	5 mm	Axial thermocouple distance Δx_{TC}	21 mm
Displacer wall thickness	1.6 mm	Gap width ratio (new seal design) r_h	0.21

[1] Please note that the gap width is substantially increased due to a similarity-based scaling procedure.

4. Results

4.1. Heat Balance

The modified laboratory-scale machine with the new seal design was subject to a comprehensive experimental plan with different rotational speeds n and mean pressures $\overline{p}$ in Stirling and Vuilleumier mode, which may be well compared to the experimental results previously obtained with the old seal design. Figure 3a shows a comparison of the experimental heat flows at nominal conditions in Vuilleumier mode for both seal designs. The results illustrate the absolute values of the heat flows and were obtained by multiple measurements on different days, and the error bars indicate the maximum differences between these measurements.

The individual experiments were performed by pressurizing the machine, selecting the operating mode, and setting the speed. After reaching steady-state operation, the measurements were performed.

The heat input to the heater, as well as the heat output at the warm temperature level and the heat input at the cold temperature level, which is called refrigeration power here in distinction to the heat input at the hot temperature level, were corrected for thermal losses to the surroundings, which were determined separately [13]. In detail, the thermal loss at the hot temperature level was determined at machine standstill by heating the hot section, evaluating the steady-state heat input, and simultaneously measuring the surface temperatures at different locations. This procedure was performed for different heater temperatures, and it was possible to derive the heat transition coefficient in dependency on the temperature difference ΔT between the heater surface and the surroundings. The heat transition coefficient was calculated as 3 W/K at ΔT = 50 K and 3.6 W/K at ΔT = 100 K. Additionally, a control calculation for natural convection at a vertical wall was performed, which yields 2.1 W/K at ΔT = 50 K. The difference can presumably be attributed to a chimney effect. During the experiments, the actual surface temperature is measured when steady-state operation is reached, and thereby the thermal loss is determined. The calculated heat loss at the hot temperature level is about 300 W to 400 W for the investigated operating conditions. Furthermore, the thermal losses at the warm and the cold temperature levels were calculated similarly. Energy conservation is thereby not always exactly fulfilled, indicating some minor remaining uncertainties. Especially the evaluation of the thermal loss at the heater is considered to be error-prone. Please note, this procedure is necessary because of the increased surface area of the experimental machine due to the scaling procedure. However, it is assumed that any systematic errors are approximately constant for all measurements. So, general statements on the effects of the new seal design are possible.

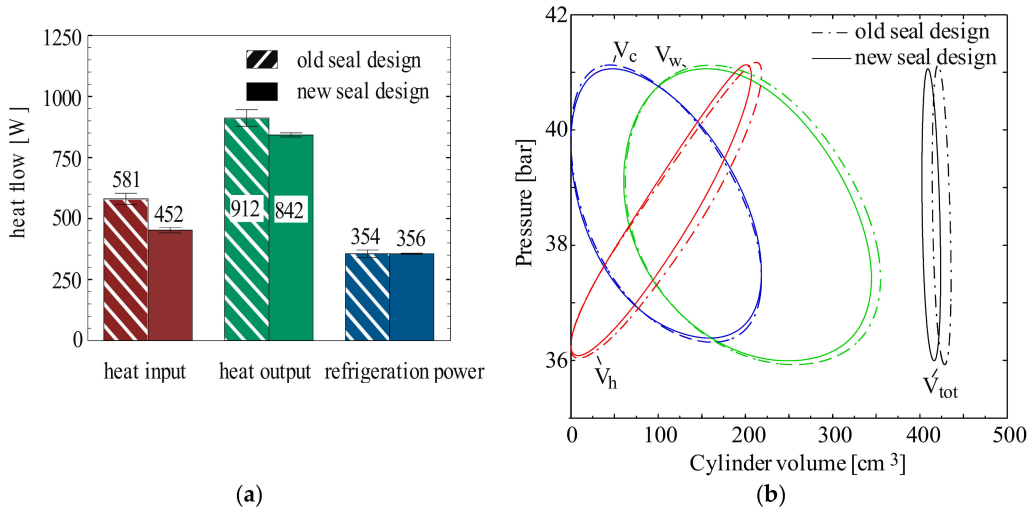

Figure 3. Experimental heat input, heat output and refrigeration power: (**a**) and p,V-plots (**b**) in Vuilleumier mode with new and old seal design at nominal conditions.

Additionally, Figure 3b shows p,V-plots for either seal design at a selected operating point. The plots are generated using the pressure data recorded at the corresponding temperature levels and neglecting any dead volumes. The pressure data are filtered by a subsequent Fourier transform with a cut-off frequency of 64 Hz, which is ten times the rotational speed. The integral values—graphically corresponding to the areas of the p,V-plots—represent both the work done and the heat absorbed by the particular volume in the case of an idealized cycle without thermal losses and may therefore be referred to as "indicated amounts of heat". The indicated work of the total cycle is the sum of these and cannot be graphically visualized by a single p,V-plot due to spatial pressure differences in the machine. Instead, the p,V-plot for the total volume V_{tot} is generated using the pressure at the warm temperature level and therefore is an approximate indication of the work done by an ideal cycle without any flow losses.

Despite the remaining uncertainties, Figure 3a clearly demonstrates that both heat input and heat output are significantly reduced by the new seal design. Simultaneously, the refrigeration power remains constant within the range of measurement accuracy. The decrease of the heat flows at the hot and warm temperature levels, which are generally the sum of the indicated heat flows and the thermal losses, may be explained by two different effects. On the one hand, it may indicate a reduction of the internal losses; e.g., the appendix gap loss, which is the intention pursued by the new seal design. On the other hand, the volumetric displacement by the hot displacer is reduced, which results in a smaller lateral width of the associated p,V-Area, and thus a smaller heat input. However, the reduced displacement typically also entails a smaller thermal expansion and compression, but surprisingly the pressure amplitude is hardly reduced only in this case.

Some theoretical considerations may help to understand the processes in the gap more clearly and to decide which of these is more likely or dominant. The main purpose of moving the displacer in a regenerative machine is to achieve a maximum thermal compression effect; i.e., a change of the cycle pressure that is solely induced by a temperature change of the displaced volume of working gas at a constant overall cycle volume. The displaced volume is typically assumed to be equal to the overall stroke volume of the displacer, including the volume displaced by the cross section of the moving seal. Now, assuming that the gas temperature is the arithmetic mean of both adjacent wall temperatures throughout the gap, the gap volume can notionally be split up into one half featuring the same temperature profile as the displacer wall and one half featuring the temperature profile of the cylinder wall. This is illustrated in Figure 4 for three different gap width ratios and for the bottom and top dead center position of the displacer. Additionally, the temperature profiles in the cylinder and displacer wall are assumed to match in the medium position of the latter. The gas quantities in the range of the gap that are displaced due to the motion of the displacer are indicated by dotted rectangles and arrows. Remarkably, only the quantity highlighted by crosshatching actually undergoes a temperature change, and the size of this gas quantity is independent of the seal design. Thus, the overall amount of gas effectively displaced between the hot and the warm temperature level is the same, regardless of the gap width ratio, and it is smaller than the overall stroke volume of the old design. Obviously, the gap is assumed to act as a perfect regenerator in the illustrated case, which will not be true in reality. However, it becomes evident that the additional thermal compression effect by the larger stroke volume in the case of the old design is marginal.

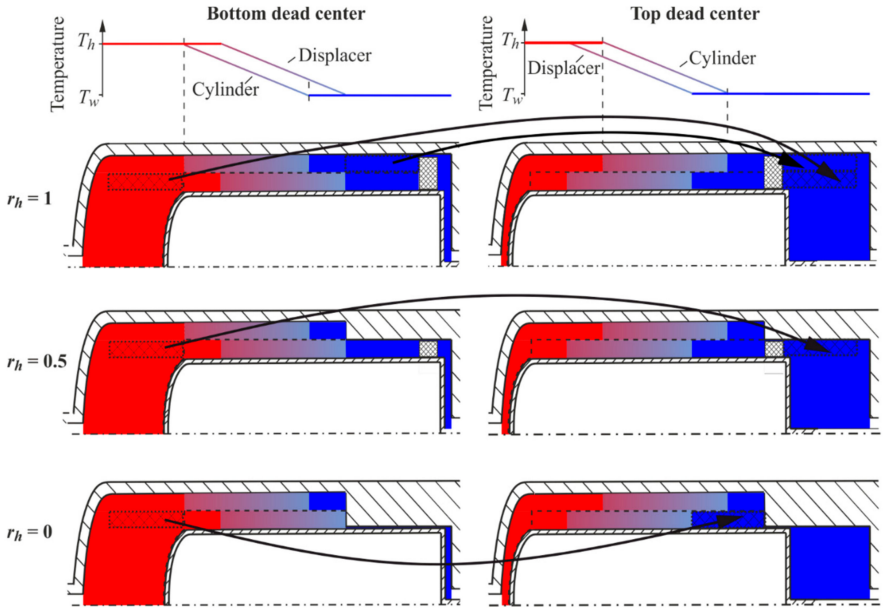

Figure 4. Temperature distribution in the cylinder system in dependency on the gap width ratio and the displacer position.

Furthermore, the overall dead volume of the machine is reduced by the design modification, as indicated by the relative lateral shift of the p,V-plots for the total volume in Figure 3b, and due to these antagonistic effects, the pressure amplitude is only marginally reduced. To some extent, this explains why the refrigeration power remains approximately constant. In detail, Figure 3b reveals that the marginal decrease of the pressure amplitude is compensated by a lateral widening of the cold loop area, which may be attributed to reduced flow losses in the hot section due to the smaller volumetric displacement, as further addressed below.

Analogically, Figure 5a shows the experimental heat flows and the indicated power of the entire cycle for both seal designs in Stirling mode, whilst Figure 5b presents the corresponding p,V-plots. The indicated power is the sum of the p,V-integrals of all three cylinder volumes multiplied by the rotational speed. Since the latter p,V-integrals are evaluated with the corresponding pressures, flow losses are included in the indicated power, which is therefore a measure for the potentially available power, disregarding mechanical losses. The results for the indicated power also include error bars, but these are smaller than line thickness. Please note, the calculated indicated power values were not affected by filtering of the pressure data.

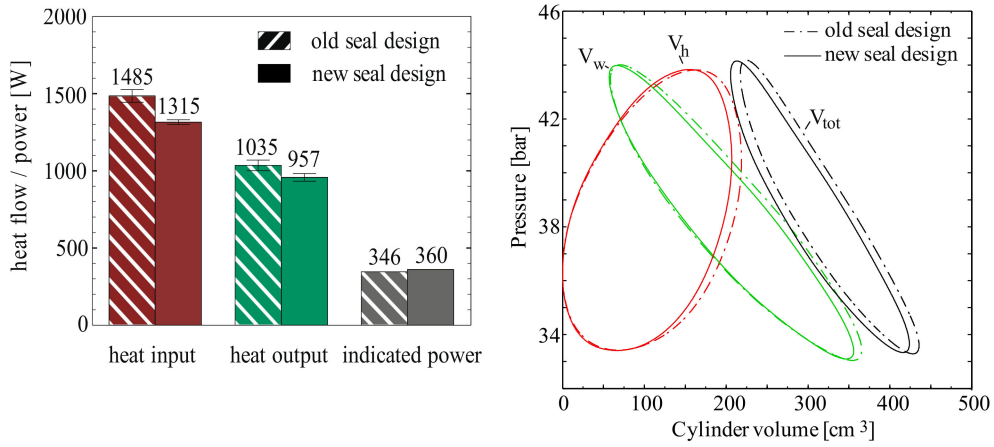

Figure 5. Experimental heat input, heat output and indicated power: (**a**) and p,V-plots (**b**) in Stirling mode with new and old seal design at nominal conditions.

Evidently, both heat input and output are significantly reduced again with the new seal design according to Figure 5a. Furthermore, Figure 5b shows that the pressure amplitudes are almost unchanged. This is not surprising since in Stirling mode the influence of a possibly decreased thermal compression is small compared to the mechanical compression by the piston, and thus less evident than in Vuilleumier mode. Furthermore, it is surprising that the indicated power is actually increased by the new seal design. This appears implausible at first sight, suggesting a measurement error due to the expectation that an unchanged pressure amplitude will yield an unchanged indicated power. However, to understand this effect, the pressure data are investigated in more detail in the following:

Figure 6 presents the pressure differences in the machine between the hot and the warm section ($p_h - p_w$), as well as between the cold and warm sections ($p_c - p_w$) for both seal designs in Vuilleumier mode (a) and Stirling mode (b). These are essentially caused by flow losses in the regenerators and the adjacent heat exchangers, which inevitably reduce the indicated power. Evidently, the pressure difference between the cold and the warm section is hardly affected by the seal design in either operating mode. In contrast, the pressure difference (i.e., the flow loss) between the hot and the warm section is clearly reduced, which is apparently due to the reduced volumetric displacement by the displacer, and which is the reason for the increased indicated power. Furthermore, the reduced mass flow through the regenerator implies a smaller reheat loss and a decrease of the regenerated amount of

heat; i.e., the thermal regenerator losses are also reduced. This additionally contributes to a reduction of the heat input and output in either operating mode. Furthermore, the reduced loads on the heater and the cooler help to raise the thermal compression effect again. So, the new seal design does not only improve the cycle performance by a direct reduction of the appendix gap loss, but also by a series of indirect positive feedback effects.

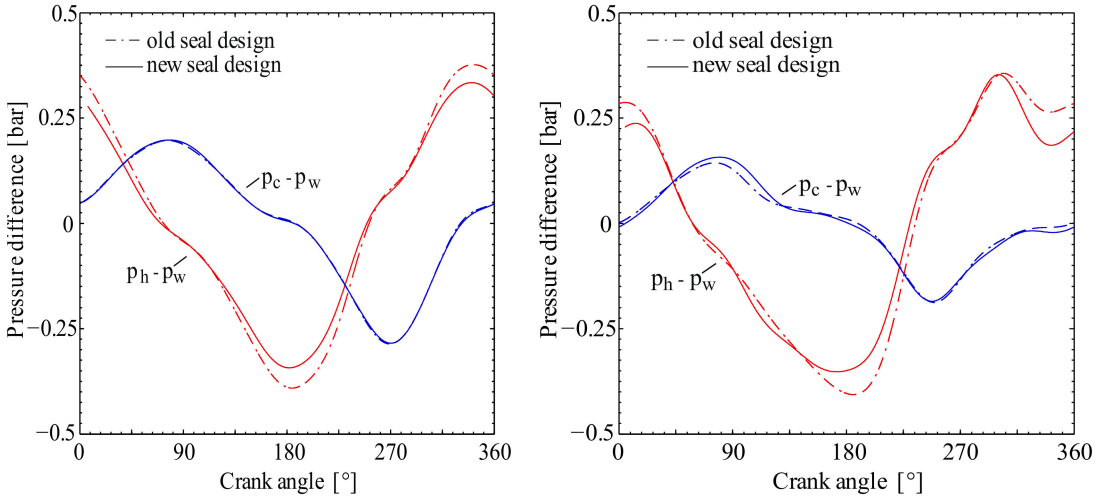

Figure 6. Measured pressure differences between the temperature levels with the old and the new seal design at nominal conditions in: (**a**) Vuilleumier mode and (**b**) Stirling mode.

4.2. Gas Temperatures

To further investigate how the new seal design affects the transport mechanisms right in the gap; the measured gas temperature profiles will be analyzed in the following: Figure 7 contrasts cyclic gas temperature fluctuations measured with the probe closest to the seal (probe d in Figure 2) at various radial positions in Vuilleumier mode with the old (a) and the new (b) seal design. The corresponding p,V-plots and axial cylinder wall temperature profiles are presented in Figure 8.

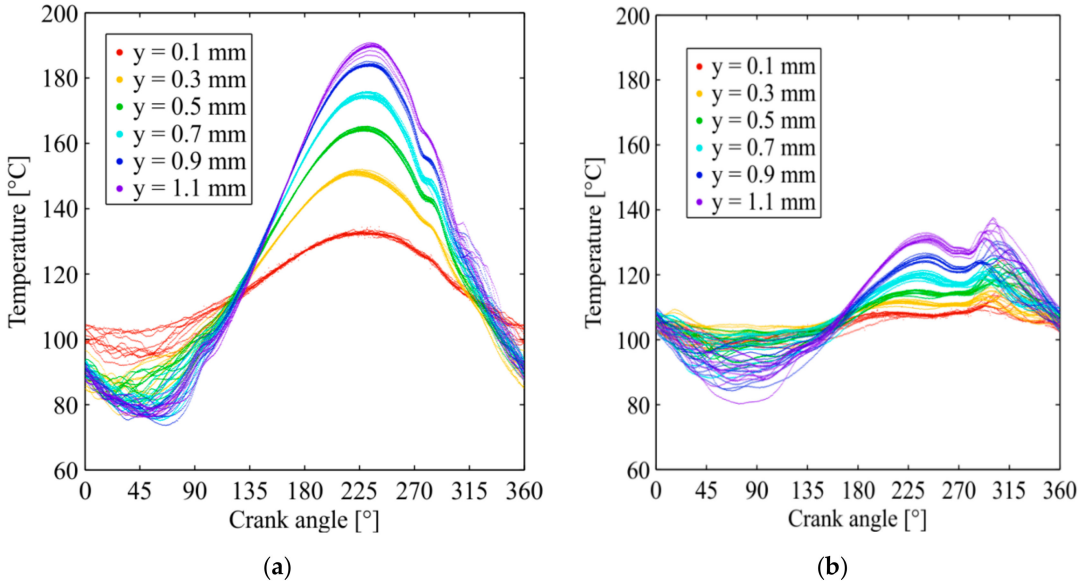

Figure 7. Gas temperatures in Vuilleumier mode close to the seal (probe d) at nominal conditions except $\overline{p}$ = 20 bar: (**a**) old seal design [32]; (**b**) new seal design.

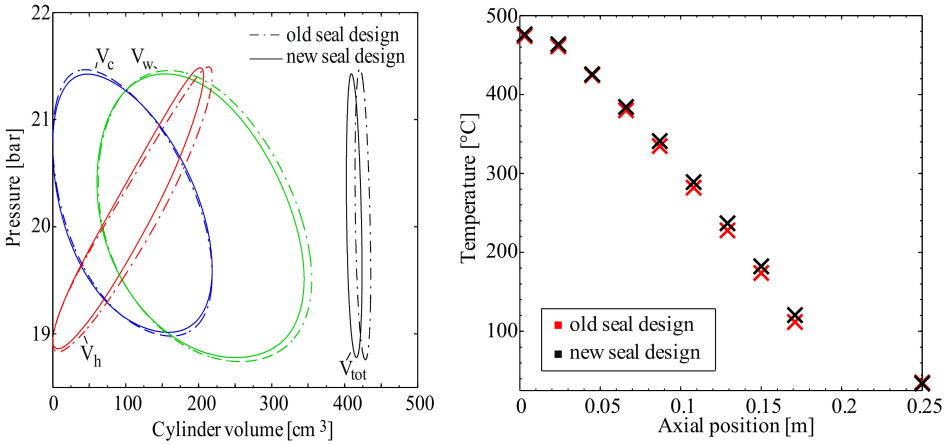

Figure 8. Measured p,V-plots (**a**) and wall temperatures (**b**) in Vuilleumier mode with new and old seal design at nominal conditions, except $\overline{p}$ = 20 bar.

According to Figure 7, the new seal design evidently yields generally smaller gas temperature fluctuations at all radial positions. Under laminar flow conditions, these are essentially induced by the axial temperature gradient in the flowing gas. Smaller gas temperature fluctuations may therefore be attributed to either a lower temperature gradient or a shorter travelling distance of the gas due to smaller flow velocities. The former explanation can be excluded in this case, since Figure 8b) illustrates that the axial wall temperature profiles, which strongly affect the gas temperature gradients, differ only marginally. These were measured by the aforementioned additional thermocouples mounted on the outer surface of the cylinder wall. The latter explanation, however, is very plausible since the volumetric displacement by the seal essentially imposes the flow velocity at the bottom end of the gap.

At the open end, the volumetric displacement is in contrast superimposed by density fluctuations of the gas in the gap, which are induced by cyclic fluctuations of both its spatial mean temperature and the cycle pressure. Due to these effects, the local flow velocity amplitudes usually increase toward the open end of the gap [26]. For the same conditions as before, Figure 9 presents the cyclic gas temperature fluctuations close to the open end (probe a in Figure 2), which are apparently reduced during the first half-cycle in the case of the new seal design, whereas during the second half-cycle, very large, stochastic fluctuations are observed for both seal designs.

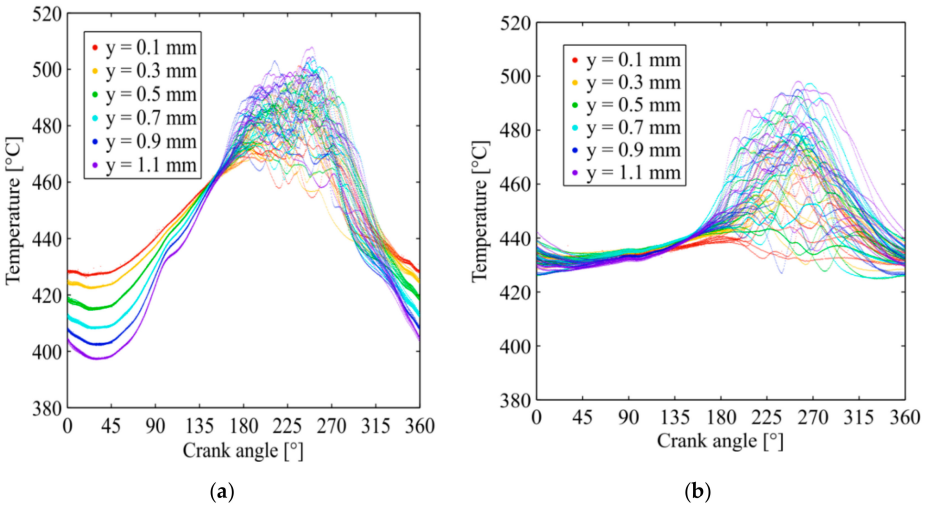

Figure 9. Gas temperatures in Vuilleumier mode at the open end (probe a) at nominal conditions except $\overline{p}$ = 20 bar: (**a**) old seal design [32]; (**b**) new seal design.

According to Sauer and Kühl [32], these fluctuations are most likely caused by turbulent eddies in the cylinder volume, which are pushed into the appendix gap beyond the location of the probe because of both pressure rise and displacer motion. They indicate turbulent flow, but contrarily to the previous case, no clear statement about reduced or increased flow velocities is possible. However, smaller gas temperature fluctuations in the first half-cycle once again indicate reduced flow velocities here, and therefore this is most likely also true during the second half-cycle. Such decreases of the gas temperature fluctuations in the gap with the new seal design are generally observed at any operating modes and conditions, as Figure 10 exemplarily illustrates for the gas temperature fluctuations close to the seal at y = 0.7 mm at various operating conditions in Stirling mode.

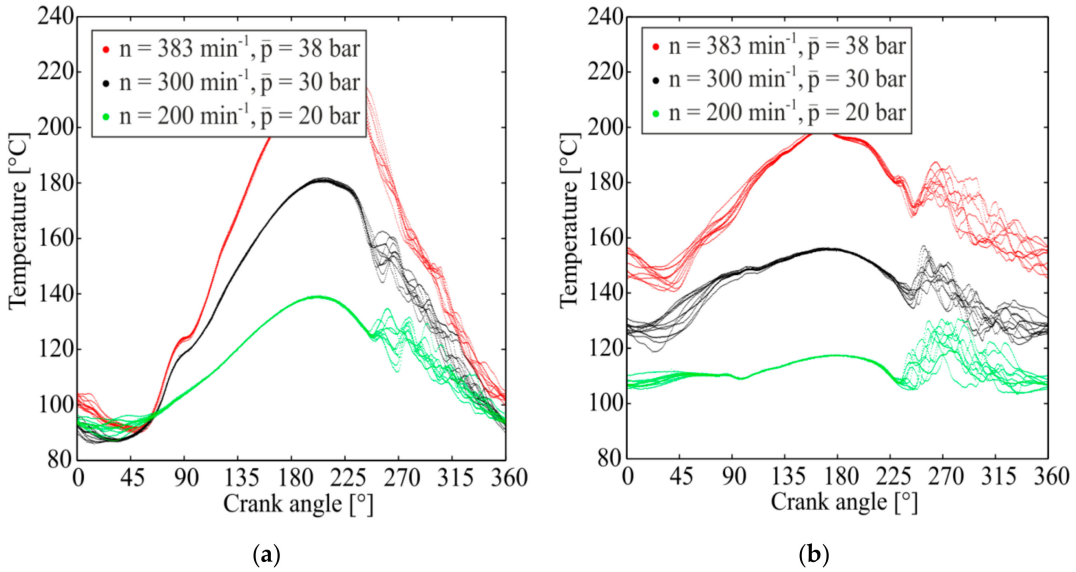

Figure 10. Measured gas temperatures in Stirling mode at different operating conditions close to the seal at y = 0.7 mm: (**a**) old seal design; (**b**) new seal design.

These results suggest that the new seal design particularly reduces the enthalpy loss since this is directly coupled to the flow velocities and gas temperature fluctuations in the gap. In contrast, it is suspected that the shuttle loss is hardly changed since this loss is coupled to the axial wall temperature profiles, which are almost the same. However, remaining open questions concerning these presumptions and the prediction of the optimum gap geometry cannot be resolved experimentally. Therefore, further theoretical and numerical investigations are needed to generalize these results and make them applicable to the design of new machines. However, these considerations shall be presented separately due to their complexity and cannot be accommodated within the scope of this contribution without rendering it unmanageable.

5. Summary

In this work, the predicted reduction of the appendix gap loss by an enhanced seal design featuring a gap width ratio $r_h < 1$ could be directly verified experimentally. It turned out that a step in the cylinder wall may improve the entire performance of the Stirling cycle, as well as the Vuilleumier cycle by several direct and indirect effects. First, the thermal loss is reduced due to smaller mass flows at the open end of the gap and thus a smaller enthalpy loss. Additionally, the volumetric displacement by the displacer is reduced, resulting in lower flow friction and thermal losses in the regenerator and its adjacent components. Contrary to initial expectations, thermal compression is at the same time hardly affected, since the gap also acts as a regenerator to some extent. However, the gas need not take the indirect route via the regenerator to achieve this regeneration effect, and thus the aforementioned flow losses, as well as the regenerator thermal losses, are in turn reduced. In detail, these effects led to

a reduction of the heat input by more than 12% in Stirling mode and by more than 28% in Vuilleumier mode whilst the power output and the refrigeration power respectively remained constant. Finally, these results suggest that the common displacer design, with an effective seal diameter equal to that of the cylinder wall in the gap above, is generally suboptimal and may possibly be improved a posteriori in many cases by retrofitting a liner and a seal with a somewhat reduced diameter. However, further studies are indispensable to derive general design rules for the optimum seal diameter; these will be presented in a subsequent contribution.

Author Contributions: Both authors contributed to the research in this paper: conceptualization, H.-D.K.; methodology, J.S. and H.-D.K.; validation, J.S. and H.-D.K.; formal analysis, J.S.; investigation, J.S.; resources, H.-D.K.; data curation, J.S.; writing—original draft preparation, J.S.; writing—review and editing, J.S. and H.-D.K.; visualization, J.S.; supervision, project administration, and funding acquisition, H.-D.K.

Funding: This research was funded by the German Research Foundation (DFG), grant number KU 755/4-1 & 2.

Conflicts of Interest: The authors declare no conflict of interest. The funders had no role in the design of the study; in the collection, analyses, or interpretation of data; in the writing of the manuscript, or in the decision to publish the results.

Nomenclature

Δ	difference
h	appendix gap width (m)
l	length (m)
n	rotational speed (min^{-1})
p	pressure (bar)
r_h	gap width ratio
T	temperature (°C)
V	Volume (m^3)
Superscripts	
$^-$	temporal average
Subscripts	
a	appendix gap
c	cold
h	hot
TC	thermocouple
tot	sum of all cylinder volumes
w	warm, intermediate

References

1. Mahkamov, K. An Axisymmetric Computational Fluid Dynamics Approach to the Analysis of the Working Process of a Solar Stirling Engine. *J. Sol. Energy Eng.* **2006**, *128*, 45–53. [CrossRef]
2. Abbas, M.; Said, N.; Boumeddane, B. Thermal analysis of Stirling engine solar driven. *Rev. Energies Renouvables* **2008**, *11*, 503–514.
3. Le'an, S.; Yuanyang, Z.; Liansheng, L.; Pengcheng, S. Performance of a prototype Stirling domestic refrigerator. *Appl. Therm. Eng.* **2009**, *29*, 210–215. [CrossRef]
4. Chen, C.L.; Ho, C.E.; Yau, H.Y. Performance Analysis and Optimization of a Solar Powered Stirling Engine with Heat Transfer Considerations. *Energies* **2012**, *5*, 3573–3585. [CrossRef]
5. Ulloa, C.; Miguez, J.-L.; Porteiro, J.; Eguia, P.; Cacabelos, A. Development of a transient model of a stirling-based CHP system. *Energies* **2013**, *6*, 3115–3133. [CrossRef]
6. Aksoy, F.; Karabulut, H.; Çınar, C.; Solmaz, H.; Özgören, Y.Ö.; Uyumaz, A. Thermal performance of a Stirling engine powered by a solar simulator. *Appl. Therm. Eng.* **2015**, *86*, 161–167. [CrossRef]
7. Qiu, S.; Solomon, L.; Rinker, G. Development of an integrated thermal energy storage and free-piston stirling generator for a concentrating solar power system. *Energies* **2017**, *10*, 1361. [CrossRef]
8. Egas, J.; Clucas, M.D. Stirling Engine Configuration Selection. *Energies* **2018**, *11*, 584. [CrossRef]

9. Ranieri, S.; Prado, A.O.G.; MacDonald, D.B. Efficiency reduction in stirling engines resulting from sinusoidal motion. *Energies* **2018**, *11*, 2887. [CrossRef]
10. Sowale, A.; Anthony, J.E.; Kolios, J.A. Optimisation of a quasi-steady model of a free-piston stirling engine. *Energies* **2018**, *12*, 72. [CrossRef]
11. Heikrodt, K.; Heckt, R. *Gasbetriebene Wärmepumpe zur monovalenten Raumbeheizung und Trinkwassererwärmung*; BMBF Final Report No. 0326947E; BVE Thermolift GbR: Aachen, Germany, 1999.
12. Kühl, H.-D.; Rüther, J.; Schulz, S. Experimental Operating Characteristics of Three Different Displacer Systems for Free Piston Vuilleumier Heat Pumps. In Proceedings of the International Stirling Forum, Osnabrück, Germany, 5–6 May 2004.
13. Geue, I.; Pfeiffer, J.; Kühl, H.D. Laboratory-Scale Stirling-Vuilleumier Hybrid System Part II: Experimental Results. *J. Propul. Power* **2013**, *29*, 812–824. [CrossRef]
14. Dogkas, G.; Rogdakis, E.; Bitsikas, P. 3D CFD simulation of a Vuilleumier heat pump. *Appl. Therm. Eng.* **2019**, *153*, 604–619. [CrossRef]
15. Rios, P.A. An approximate solution to the shuttle heat-transfer losses in a reciprocating machine. *J. Eng. Gas. Turb. Power* **1971**, *93*, 177–182. [CrossRef]
16. Chang, H.M.; Park, D.J.; Jeong, S. Effect of gap flow on shuttle heat transfer. *Cryogenics* **2000**, *40*, 159–166. [CrossRef]
17. Berchowitz, D.; Berggren, R. *Appendix Gap Losses in Reciprocating Machines*; MTI Report No. 81ASE187ER16; Mechanical Technology Incorporated: Latham, NY, USA, 1981; p. 27.
18. Magee, F.N.; Doering, R.D. *Vuilleumier-Cycle Cryogenic Refrigeration Development*; AFFDL-TR-68-67; Air Force Flight Dynamics Laboratory, Wright-Patterson Air Force Base: Greene County, OH, USA, 1968.
19. Andersen, S.K.; Carlsen, H.; Thomsen, P.G. Preliminary results from a numerical study on the appendix gap losses in a Stirling engine. In Proceedings of the 12th International Stirling Engine Conference, Durham, NC, UK, 7–9 September 2005; pp. 336–347.
20. Sauer, J.; Kühl, H.D. Numerical model for Stirling cycle machines including a differential simulation of the appendix gap. *Appl. Therm. Eng.* **2017**, *111*, 819–833. [CrossRef]
21. Nishio, S.; Inada, T.; Nakagome, H. Shuttle Heat-Transfer in Refrigerators. In *Transport Phenomena in Thermal Engineering*; Su, J.S., Chung, S.H., Kim, K.H., Eds.; Begell House: Danbury, CT, USA, 1993; pp. 484–489.
22. Huang, S.C.; Berggren, R. Evaluation of Stirling Engine Appendix Gap Losses. In Proceedings of the 21st Intersociety Energy Conversion Engineering Conference, San Diego, CA, USA, 25–29 August 1986; pp. 562–568.
23. Zimmerman, F.J.; Longsworth, R.C. Shuttle Heat Transfer. In *Proceedings of the Cryogenic Engineering Conference, Boulder, CO, USA, 17 June 1970*; Advances in Cryogenic Engineering; Springer: Boston, MA, USA, 1971; Volume 16, pp. 342–351.
24. Harness, J.B.; Newmann, P.E.L. A Theoretical Solution of Shuttle Heat Transfer Problem. In Proceedings of the 4th International Cryogenic Conference, Eindhoven, The Netherlands, 24–26 May 1972; pp. 97–100.
25. Mabrouk, M.T.; Kheiri, A.; Feidt, M. Effect of leakage losses on the performance of a β type Stirling engine. *Energy* **2015**, *88*, 111–117. [CrossRef]
26. Pfeiffer, J.; Kühl, H.-D. New Analytical Model for Appendix Gap Losses in Stirling Cycle Machines. *J. Thermophys. Heat Trans.* **2016**, *30*, 288–300. [CrossRef]
27. Pfeiffer, J.; Kühl, H.D. Optimization of the Appendix Gap Design in Stirling Engines. *J. Thermophys. Heat Trans.* **2016**, *30*, 831–842. [CrossRef]
28. Thieme, L.G. *Low-Power Baseline Test. Results for the GPU 3 Stirling Engine*; NASA-TM-79103; NASA Lewis Research Center: Cleveland, OH, USA, 1979.
29. Thieme, L.G.; Tew, R.C., Jr. *Baseline Performance of the GPU-3 Stirling Engine*; NASA TM-79038; NASA Lewis Research Center: Cleveland, OH, USA, 1978.
30. Geue, I. Entwicklung, ähnlichkeitstheoretische Skalierung und Untersuchung eines umschaltbaren Systems aus Stirlingmotor und Vuilleumier-Wärmepumpe zur dezentralen Hausenergieversorgung. Ph.D. Thesis, Chair of Thermodynamics. TU Dortmund University, Dr. Hut, München, Germany, 2012.
31. Kühl, H.-D.; Pfeiffer, J.; Sauer, J. Operating Characteristics of a Laboratory-Scale, Convertible Stirling-Vuilleumier-Hybrid CHP System Including a Reversed-Rotation Stirling Mode. In Proceedings of the 16th International Stirling Engine Conference, Bilbao, Spain, 24–26 September 2014; pp. 294–304.

32. Sauer, J.; Kühl, H.D. Analysis of unsteady gas temperature measurements in the appendix gap of a stirling engine. *J. Propul. Power* **2018**, *34*, 1039–1051. [CrossRef]
33. Pfeiffer, J.; Kühl, H.D. Review of Models for Appendix Gap Losses in Stirling Cycle Machines. *J. Propul. Power* **2014**, *30*, 1419–1432. [CrossRef]
34. Geue, I.; Kühl, H.D. Design of a Convertible Stirling—Vuilleumier Hybrid System for Demand-oriented Decentralized Cogeneration and Heat Pump Application. In Proceedings of the International Stirling Forum, Osnabrück, Germany, 23–24 September 2006.
35. Geue, I.; Pfeiffer, J.; Hötzel, J.; Kühl, H.D. Design of an Experimental Convertible Stirling-Vuilleumier Hybrid System Obtained by Similarity-Based Scaling. In Proceedings of the 14th International Stirling Engine Conference, Groningen, The Netherlands, 16–18 November 2009.
36. Geue, I.; Pfeiffer, J.; Kühl, H.D. Laboratory-scale stirling-vuilleumier hybrid system part i: Application of similarity-based design. *J. Propul. Power* **2013**, *29*, 800–811. [CrossRef]